

Cerium-Based, Intermetallic-Strengthened Aluminum Casting Alloy: High-Volume Co-product Development

ZACHARY C. SIMS,¹ D. WEISS,² S.K. MCCALL,³ M.A. MCGUIRE,¹
R.T. OTT,⁴ TOM GEER,¹ ORLANDO RIOS,^{1,5} and P.A.E. TURCHI³

1.—Oak Ridge National Laboratory, Oak Ridge, TN, USA. 2.—Eck Industries, Manitowoc, WI, USA. 3.—Lawrence Livermore National Laboratory, Livermore, CA, USA. 4.—Ames National Laboratory, Ames, IA, USA. 5.—e-mail: orios@ornl.gov

Several rare earth elements are considered by-products to rare earth mining efforts. By using one of these by-product elements in a high-volume application such as aluminum casting alloys, the supply of more valuable rare earths can be globally stabilized. Stabilizing the global rare earth market will decrease the long-term criticality of other rare earth elements. The low demand for Ce, the most abundant rare earth, contributes to the instability of rare earth extraction. In this article, we discuss a series of intermetallic-strengthened Al alloys that exhibit the potential for new high-volume use of Ce. The castability, structure, and mechanical properties of binary, ternary, and quaternary Al-Ce based alloys are discussed. We have determined Al-Ce based alloys to be highly castable across a broad range of compositions. Nanoscale intermetallics dominate the microstructure and are the theorized source of the high ductility. In addition, room-temperature physical properties appear to be competitive with existing aluminum alloys with extended high-temperature stability of the nanostructured intermetallic.

INTRODUCTION

Increasing demand for Ce will indirectly impact rare earth (RE) based permanent magnets and phosphors used for efficient lighting by helping to stabilize RE production.¹ The major economic concern with currently available high-performance permanent magnets is the availability and sensitivity to price fluctuations. Technologies that increase the demand for cerium and lanthanum can make the continued production of more high-value REs economically viable, alleviating some of the pressure associated with modern permanent magnet manufacturing. In this contribution, we describe a potential high-volume use for Ce in the aluminum castings industry. The development of high-temperature aluminum cerium alloys will provide a material solution enabling the design of higher efficiency internal combustion engines and lighter drive trains, improving fuel economy.

The economic impact could be significant with even partial adoption of this technology. Two million metric tons of aluminum are consumed annually in transportation. For every 1% of aluminum

transportation market penetration, assuming a 12 wt.% Ce alloy, 2400 t of cerium would be required, with global production of Ce of about 24,000 t annually. High-performance aluminum is a dynamic market that quickly responds to technological innovations. The commercialization path in part will depend on the cost of cerium. At an alloy cost of less than \$10.00/kg, there could be significant interest and adoption by the automotive industry. The high strength could result in lighter weight components and significant adoption in applications requiring good high-temperature strength. At alloy costs in the \$10 to \$20 range, commercialization activities would concentrate on military application, where the alloy strength could be used advantageously for lighter weight structures. At alloy costs greater than \$20/kg, commercialization activity would concentrate on the commercial, general aviation, and space markets where strength and high-temperature performance would be justified by the high penalty of weight. Where high-temperature performance would normally be addressed by the conversion of aluminum to titanium, much higher prices may be justified. The evidence suggests that as much as 25% to 30% of the

existing titanium market (4000 t annually) is driven by temperature performance in the 150°C to 315°C range, which is within the expected operating range of this alloy system.²

In the early 1980s, some promising research and development efforts focused on powder metallurgy revealed that aluminum alloys containing 4 wt.% cerium exhibit high-temperature mechanical properties that exceed the best commercial aluminum casting alloys currently in production. Even though these alloys had both high room and elevated temperature strengths, work did not continue due to cerium cost and supply challenges coupled with the limited applicability of powder metallurgy in near net shape forming of aluminum components. Aluminum cerium alloy components prepared via hot pressing and forging exhibited tensile strengths of 300 MPa at 230°C.³ This compares to typical tensile strengths of 70–180 MPa for Al-Cu and Al-Mg-Zn systems at that temperature.⁴ High Ce content Al alloys have not been developed for casting nor have the casting characteristics been determined.

The successful development of this alloys will have broad technological impact. The breadth of which will include economic effects on materials for alternative energy technologies such as Nd and Dy and the fossil fuel dominated transportation sector. High Ce level aluminum alloys could assist in stabilizing the price of the heavier RE elements that are most important to green energy. The enhanced properties enabled by Ce additions to aluminum are expected to be attractive in the transportation sector. This work may lead to the development of new high-temperature aluminum alloys suitable for applications such as automotive cylinder heads, turbo charger housings, and impellers. Mechanical property improvements of 20% to 40% at high temperatures enhance the thermodynamic efficiency of end products such as internal combustion engines leading to reductions in fuel consumption while enabling more extensive use of castable lightweight materials. Additionally, the enhanced high-temperature, mass-specific mechanical properties can be used to manufacture lighter drive trains and expand the use of lightweight materials in commercial transport vehicles such as tractor trailers.

In this article, we report results obtained during an investigation of castability of aluminum cerium alloys and determine compositional modifications that may be required to ensure the compatibility of the alloy with near net shape casting methods such as advanced sand casting, die casting, and permanent mold squeeze casting. The aluminum casting industry is an integral part of a performance-driven market segment that immediately responds to improved properties by early adaptation of technological innovations. Successful alloy development and demonstration of enhanced high-temperature mechanical properties is expected to lead to rapid commercialization in the high-performance

segment. Followed by wide-scale adaptation by more cost-driven markets such as automobile manufacturers; where there is a constant push for higher efficiency. One of the most obvious ways to improve efficiency is to reduce weight. Although many powertrain components are already produced by aluminum casting, increases in specific output driven by turbocharging and new direct fuel injection concepts have led to an increase in thermal and mechanical loads on engine components. Maximum temperatures can locally exceed 270°C in the flame deck for high specific output heads, diesel heads, and heads with integrated exhaust manifolds. Conventional aluminum alloys such as 356 and 319 have lower mechanical properties at elevated temperatures.^{4,5} This efficiency tradeoff is problematic when trying to increase the efficiency of an engine above a threshold value. What is needed is a lightweight aluminum alloy that maintains its mechanical properties at high temperatures.

The heaviest components of heavy-duty diesel engines are cast iron heads and blocks. Replacing these with a lightweight alternative would yield appreciable increases in efficiency resulting from the reduced weight. Although some aluminum alloys exist that have stable mechanical properties at high temperatures, such as the Al-Sc system, they remain cost prohibitive.^{6,7} It is then of great interest to design an alloy for use with existing aluminum casting practices that is both mechanically stable at high temperatures and sufficiently economical for application in modern engines. In this article, we show that by increasing the cerium content to 12 wt.%, it is possible to create an alloy compatible with modern casting practices with the potential to meet these needs.

EXPERIMENTAL PROCEDURES

Al-Ce alloys were cast in binary composition of 6–16 wt.% Ce. Commercially pure aluminum ingots were melted and held at approximately 785°C. Ternary and quaternary alloys with small Si and Mg additions were also investigated. In the case of the binary and ternary alloy, cerium was added last and melt was allowed to return to temperature. The quaternary alloy was poured from the remaining heel of the alloy below. During cerium addition, a highly exothermic reaction was observed with the melt temperature rising almost 25°C in 5 min. This temperature increase is correlated with strong associative interactions between the Al and Ce atoms resulting in a high enthalpy of mixing that is typically associated with the formation of intermetallic compounds during solidification.⁸ The total mass of each melt was approximately 25 kg, and castings were poured into polymer bound sand molds at 785°C.

The quaternary alloy was made from the already formed ternary alloy. The alloy most compatible with existing casting practices is Al-12Ce, where the number preceding the alloying element is its

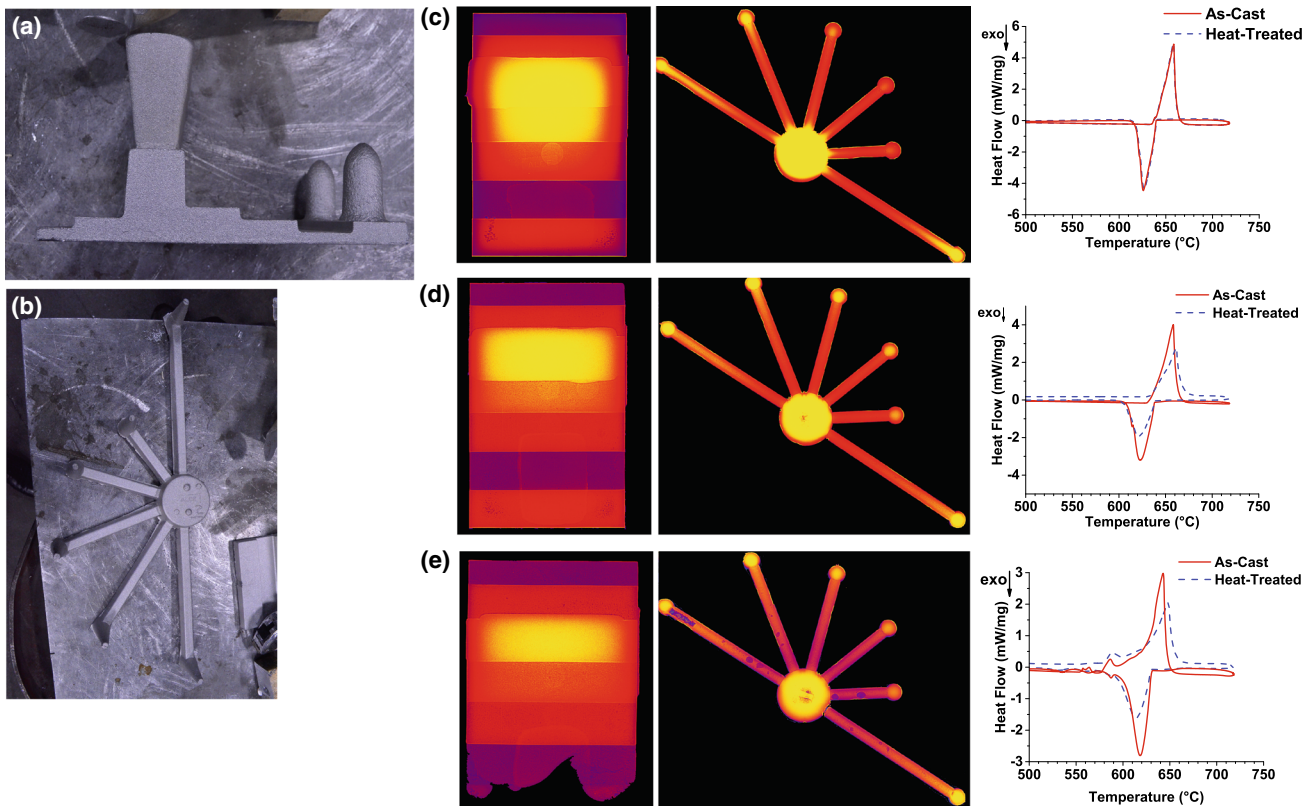


Fig. 1. (a) Casting of step-plate used in castability assessment. (b) Casting of hot-tear mold used in castability assessment. (c) Low-energy x-ray color maps of Al-12Ce hot-tear and step-plate molds with DSC curves. (d) Low-energy x-ray color maps of Al-12Ce-0.4Mg hot-tear and step-plate molds with DSC curves. (e) Low-energy x-ray color maps of Al-12Ce-4Si-0.4Mg hot-tear and step-plate molds with DSC curves.

concentration in weight percent. We will focus on three alloys in this report: Al-12Ce, Al-12Ce-0.4Mg, and Al-12Ce-4Si-0.4Mg. After casting, test bars were heat-treated to determine the effectiveness of heat-treatment on mechanical properties. A standard T6 schedule was used; test-bars were heated to 537°C and held for 8 h. After this solutionizing step, the bars were water quenched and artificially aged at 155°C for 3 h.

Castability

The castability of an alloy is related to melt fluidity, solidification shrinkage, and mechanical properties—specifically, ductility along with other thermodynamic parameters such as liquidus and solidus temperatures, partitioning coefficients, and reactivity with the mold.⁹ Hot tearing is a defect frequently encountered in all casting alloys and is severely detrimental to mechanical properties obtained from the cast component. The physical properties that lead to this behavior are complex; however, the most clearly identifiable feature defining castability is the propensity for hot tearing. These solidification-induced defects can result in part rejection, costly evaluation of individual components, and stringent control of casting parameters. The terms *gate*,

runner, *riser*, and *casting* are typically used in the description of castings and are defined in the ASM Casting Handbook.⁹

To obtain a quantitative assessment of castability and to perform an accurate comparison with commercial casting alloys, variable cooling rate tests also known as step molds were cast. A step mold shown in Fig. 1a is used to produce multiple cross-section castings that vary the mold surface to casting volume ratio. The thin sections furthest from the riser solidify at cooling rates exceeding 500°C/s while the thicker sections adjacent to the riser cool at modest rates of approximately 300°C/min. A thin section midway between the riser and the furthest section of the casting is used to provide restricted feeding of liquid metal to the furthest edge of the casting. A similarly sized thin section is attached adjacent to the riser to assure maximum feeding of the casting during solidification. Comparison of the oppositely located regions provides an assessment of castability.

Alloys were also cast into 6 arm hot-tear molds shown in Fig. 1b that were designed to vary the length of the gating between the riser and the casting at the end of each arm. The shortest arm (less than 8 cm) will easily transfer heat and molten metal from the riser to the end of the gate as opposed to the longest arm (longer than 20 cm).

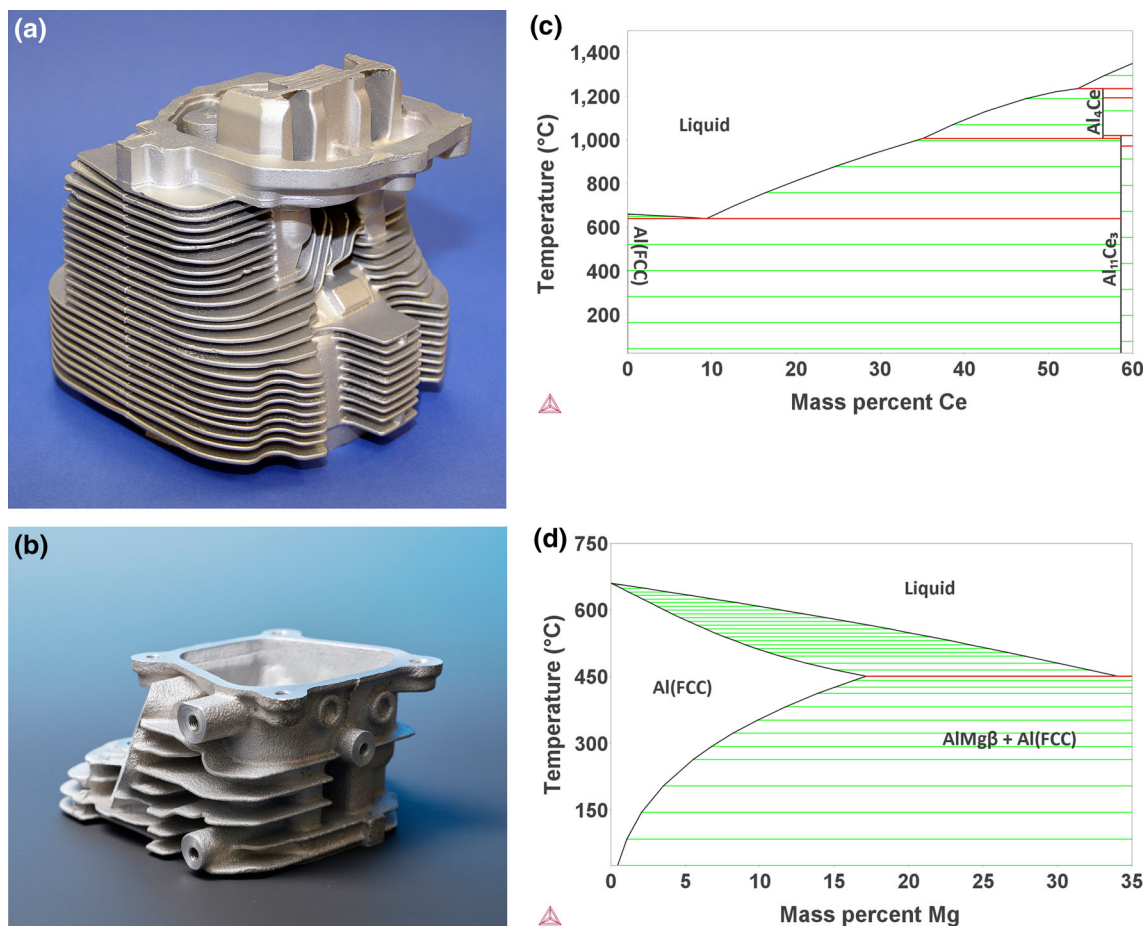


Fig. 2. (a) Air-cooled cylinder head cast from Al-12Ce. (b) Air-cooled cylinder head cast from Al-12Ce-0.4Mg. (c) Binary phase diagram of the Al-Ce system. (d) Binary phase diagram of the Al-Mg system.

Evaluation of the defect density across the various length arms enables an assessment of castability and a meaningful comparison of the propensity for hot tearing between alloys cast into similar molds. Both the step plate and hot tear castings were examined with x-ray imaging shown in Fig. 1c–e.

Figure 1 details the results of the castability study along with differential scanning calorimetry (DSC) of heating and cooling through the solidus and liquidus temperatures for the three casting alloys included in this report. DSC measurements were recorded using a Netzsch STA 4493F3 combination DSC and thermogravimetric analysis. Samples were started from room temperature, heated at 20°C/min to 750°C, and then cooled at the same rate. The binary Al-12Ce exhibits exceptional castability. The hot-tear and step-plate molds fill completely with no detectable macroscopic defects (larger than 500 μm) present in the mold. This exceptional castability is linked to a combination of increased melt fluidity and the near isothermal solidification of the Al-12Ce alloy.

Melt fluidity is strongly dependent on enthalpy of formation.¹⁰ Formation of the Al-Ce intermetallic phases is strongly exothermic. The exothermic

reaction observed after the addition of Ce to the melt could then be related to the increase in melt fluidity and, thus, to high castability. We determined that the castability of the Al-12Ce base alloy met or exceeded the castability of commercial aluminum silicon casting alloys.¹¹ This increase in melt fluidity allows the alloy to successfully fill complex molds such as the air-cooled cylinder-head pictured in Fig. 2a, cast from Al-12Ce alloy.

Mg is commonly used as a strengthening addition in aluminum alloys,^{4,11} so it was selected as a ternary additive to the Al-Ce system. As expected, castability was not impaired after an addition of only 0.4 wt.% Mg. Very few voids were observed in the x-ray images of the hot-tear and step-plate molds. Additionally, no hot-tearing is present in the molds. In comparison to the binary Al-12Ce alloy, castability is improved with the end constraints and arms of the hot-tear mold, and the edges of the step-plate molds showing greater aluminum density. Looking at the DSC curve for Al-12Ce-0.4Mg and comparing it to the curve for Al-12Ce, few differences were noted. A very sharp solidification peak, only 20°C in width, remains, and no features were discernable after solidification. However, very close

inspection of the region just before solidification shows the onset of a small exothermic reaction. This feature of the DSC curve is discussed in greater detail in the microstructure analysis to follow. The similarity between the two DSC curves implies that Mg does not significantly affect the thermodynamics or phase constitution of the Al-Ce binary system, but instead, it strengthens the matrix phase by forming intermetallic Al-Mg precipitates and metastable clusters. Intermetallic precipitates are beneficial for increasing the strength of the ductile aluminum matrix without affecting the existing $\text{Al}_{11}\text{Ce}_3$. The high castability of the Al-12Ce-0.4Mg enables complex geometry castings similar to those of the Al-12Ce. The smaller air-cooled cylinder head, shown in Fig. 2b, was cast from ternary intermetallic Al-12Ce-0.4Mg and will be used to assess the applicability of Al-Ce-X alloys to engine and motor applications in the near future.

Considering the success of ternary Mg additions, investigation into quaternary additions of Si was begun. Silicon has two effects when added to conventional aluminum alloys: Silicon works to increase alloy castability, and silicon, when combined with Mg normally precipitates a Mg_2Si strengthening phase.^{12,13} In the casting of Al-12Ce-4Si-0.4Mg, the melt was prepared from the heel left after pouring the Al-12Ce-0.4Mg. Then additional Al was added followed by Mg, Ce, and Si. During the addition of Cerium to the molten Al-Si-Mg mixture, an endothermic reaction occurred and the melt temperature dropped significantly, $\sim 30^\circ\text{C}$. The cause of the endothermic drop in temperature is unclear. This is in contrast to the normally exothermic reaction of the previous two alloys upon the addition of cerium. Once the melt was brought back to $\sim 785^\circ\text{C}$, the molten alloy was poured as before into a hot-tear and step-plate mold. Figure 1e shows the results of casting trials of an Al-12Ce-4Si-0.4Mg alloy. Silicon greatly inhibits the castability of the Al-Ce-X system. The step-plate mold did not completely fill but instead was stopped by a solidification front that nucleated on top of the iron chill. In the case of the hot-tear mold, a large number of voids is present and a hot-tear is present at the base of the right-most arm. Observing the DSC curve for the quaternary alloy, it is clear that the alloy does not solidify isothermally and is not free of secondary reactions after the initial solidus peak. However, in the case of Al-Ce-X alloys, it would appear that high silicon content impairs the castability in contention with typical silicon aluminum results.

Microstructure

Figure 2c and d shows binary phase diagrams for the Al-Ce and Al-Mg systems. These two diagrams aided in the decisions regarding compositions and melt temperature. After the finalized decisions on composition were made, test bars were cast for each alloy. Test bars are cast in a permanent steel mold.

Final bars are approximately 25 cm long and weigh ~ 0.25 kg. Disks 2 mm thick were cut from the neck of test bars prepared from each alloy. Once cut, the phase fractions of each sample were measured using a Panalytical X'pert Pro powder diffractometer. Rietveld refinement was used to determine phases and phase fractions. After x-ray diffraction (XRD), a second set of disks were polished and lightly etched with Keller's reagent. Polished samples were imaged in a Hitachi S-4700 scanning electron microscope. Figure 3 shows the images of the as-cast samples adjacent to heat-treated samples of the same composition along with XRD patterns for each alloy.

In the case of the binary Al-12Ce alloy (Fig. 3a), two phases are present: aluminum metal (gray) and the binary intermetallic $\text{Al}_{11}\text{Ce}_3$ (white). The binary intermetallic, in the as-cast state, is characterized by a highly interconnected eutectic microstructure. The XRD reveals $\text{Al}_{11}\text{Ce}_3$ is orthorhombic with lattice parameters: $a = 4.395$, $b = 10.09$, and $c = 13.025$ Å in good agreement with literature values.¹⁴ Since 12 wt.% Ce falls above the eutectic point, 10 wt.% Ce, and in the primary solidification zone for the $\text{Al}_{11}\text{Ce}_3$ intermetallic, observation of primary crystallization is expected. However, no primary crystallization is observed. Al-12Ce then undercools beyond the primary zone and solidifies in a coupled eutectic growth resulting in no primary growth and high phase fraction of the eutectic intermetallic. Moving to the heat-treated binary sample, it is clear that the morphology of the microstructure has changed. The interconnected lath-like structure has been replaced with a more independent particle-like structure. Although the structure has changed, XRD data show the phase fractions remain unaffected, resulting from the near zero solubility of cerium in aluminum. The stability of the microstructure phase constitution under high temperatures offers promise toward future high-temperature mechanical properties.

The ternary Al-12Ce-0.4Mg alloy is shown in Fig. 3b. In the as-cast state, there are primary crystals of Al_3Mg_2 consisting of large cubic grains and the $\text{Al}_{11}\text{Ce}_3$ intermetallic in both the eutectic lath microstructure and the primary crystals. The lattice parameter for the Al-Mg cubic phase is $a = 2.82$ Å.¹⁵ These crystals are not representative of the bulk microstructure, and image analysis suggests they account for roughly 1% of the areal fraction. This low fraction explains the absence of the Al_3Mg_2 from the XRD phase fraction analysis. The Al_3Mg_2 crystals remain after heat-treatment in roughly the same fraction. Mg appears to suppress the undercooling characteristics of the rapid solidification and force some small amount of primary solidification in the $\text{Al}_{11}\text{Ce}_3$ phase. The small amount of primary solidification is observable in the DSC curve just prior to the sharp onset of eutectic solidification. The eutectic microstructure is not affected by the new solidification

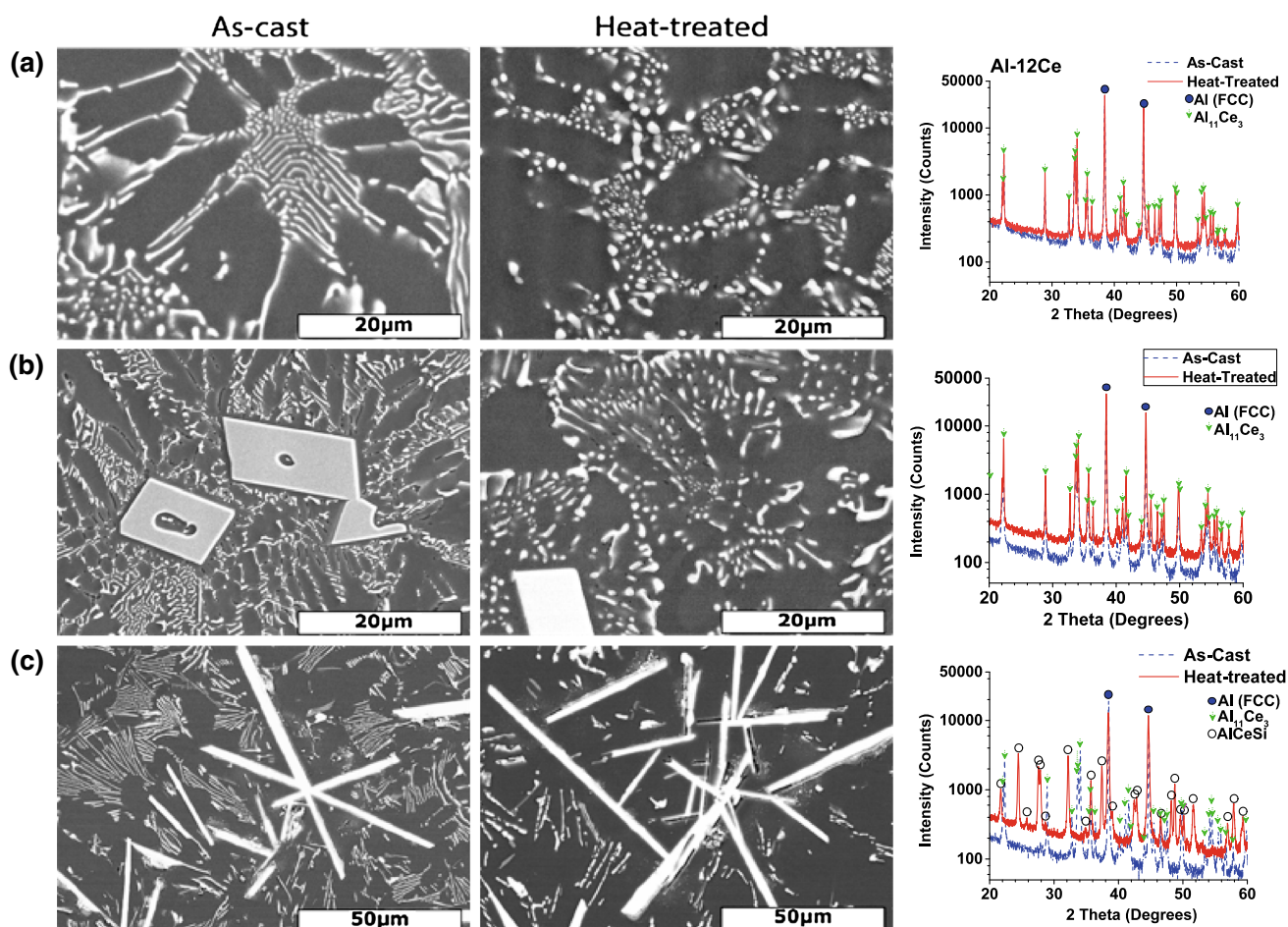


Fig. 3. (a) As-cast and heat-treated SEM images of Al-12Ce with accompanying XRD spectra and phase information. (b) As-cast and heat-treated SEM images of Al-12Ce-0.4Mg with accompanying XRD spectra and phase information. (c) As-cast and heat-treated SEM images of Al-12Ce-4Si-0.4Mg with accompanying XRD spectra and phase information.

characteristics. In the as-cast state, it remains highly interconnected with very thin laths. After heat-treatment, the same transition in the eutectic structure is observed. The finer laths have separated to form particle-like independent structures. The intermetallic particles present after heat-treatment are similarly sized to the laths present in the as-cast microstructure, and XRD shows that no phase transition has occurred with the as-cast and heat-treated spectra appearing nearly identical. The small amount of coarsening in the eutectic microstructure contrasts the ease with which Al-Si alloys coarsen after very little exposure to high temperatures.¹⁶ The thermal stability of the phase fraction and grain size are important factors in considering whether Al-Ce-X alloys have the possibility to function at higher temperatures.

The quaternary Al-12-4Si-0.4Mg alloy stands out from the binary and ternary alloys in microstructure morphology, phase constitution, and heat-treatment results. The Al-12Ce-4Si-0.4Mg alloy exists in the as-cast state as three phases. The smallest is AlSiMg accounting for less than 2 wt%.

The main two phases present are the aluminum (FCC) phase and the intermetallic Al₁₁Ce₃, both reflected in Fig. 3c. Al₁₁Ce₃ shows both primary and eutectic solidification in the as-cast state. The silicon not accounted for in AlSiMg is dissolved in the aluminum matrix. After the T6 heat-treatment, a new phase precipitates. The new phase is a ternary intermetallic, AlCeSi. This phase is tetragonal with lattice parameters $a = 4.24$, $c = 14.538$ Å consistent with published values.¹⁷ During heat-treatment, the new ternary phase consumes the eutectic growth and transforms the present primary crystals into AlCeSi.

Magnetism

Since cerium often contains a partially filled 4f electron shell, it may impart a magnetic response to its alloys and compounds. As a result, the magnetic properties can help characterize the Al-Ce alloys studied here. Here the magnetization of three binary specimens (Al-xCe $x = 6, 12$, and 16) was measured.

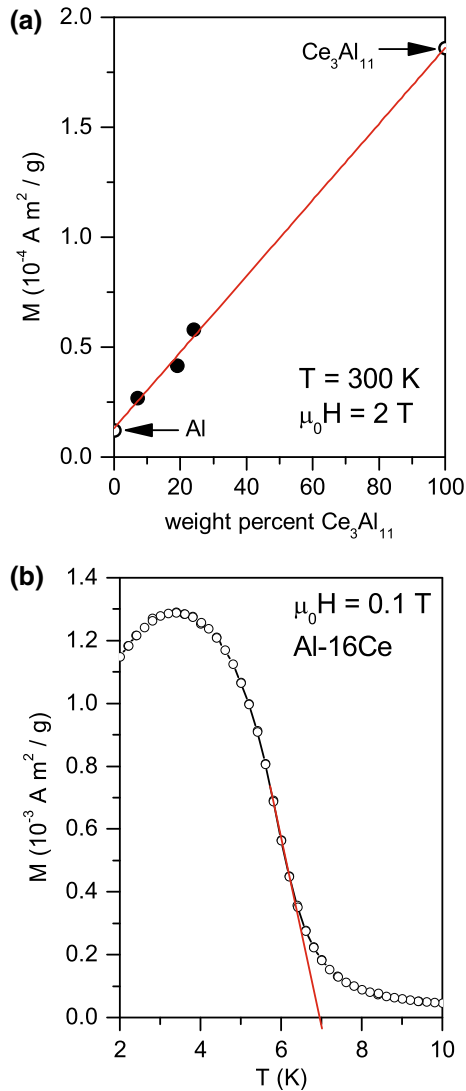


Fig. 4. (a) Magnetic moment per gram of Al, $\text{Al}_{11}\text{Ce}_3$, and three alloys at 300 K in an applied field of 2 T, with a linear fit. (b) Low-temperature magnetization of Al-16Ce showing the onset of ferromagnetism in the $\text{Al}_{11}\text{Ce}_3$ component near 7 K as estimated by the red line, and a second magnetic transition at lower temperatures.

The magnetic moment per gram at 300 K for the three alloys is shown in Fig. 4a. The data are plotted as a function of the $\text{Al}_{11}\text{Ce}_3$ content determined from the XRD refinements. The measured data closely follow the linear trend between the end members Al and $\text{Al}_{11}\text{Ce}_3$, which is consistent with a simple mixture of the two paramagnetic phases. The red line (color is shown online only) on Fig. 4a is a linear fit of five data points extrapolated to the abscissa. The magnetic susceptibility exhibits Curie behavior ($M/H \sim C/T$, where C is the Curie constant) typical of local magnetic moments. Below about 10 K, the susceptibility increases sharply (Fig. 4b). Measurements at lower temperatures reveal ferromagnetic ordering with a Curie temperature near 7 K in Al-16Ce. A downturn below about 3.5 K suggests a transition away from a simple ferromagnetic state at

lower temperatures. The observed temperature dependence is consistent with literature reports for $\text{Al}_{11}\text{Ce}_3$, which is known to have a ferromagnetic transition at 6.3 K and a ferromagnetic to antiferromagnetic transition at 3.2 K.¹⁸ The magnetic moment per gram measured at 2 K in an applied field of 5 T is $0.0030 \text{ Am}^2/\text{g}$ (3.0 emu/g). The reported average moment for $\text{Al}_{11}\text{Ce}_3$ at this temperature and field is $0.0108 \text{ Am}^2/\text{g}$ (10.8 emu/g). This indicates a concentration of 28 wt.% $\text{Al}_{11}\text{Ce}_3$ in the Al-16Ce alloy, similar to the XRD result (24 wt.%).

The measured values of the moment at 2 K and the susceptibility at 300 K support the presence of $\text{Al}_{11}\text{Ce}_3$ as the primary Ce containing phase in the tested Al-Ce alloys, and the temperature dependence and transition temperatures indicates this phase is present in well-ordered grains that behave similarly to bulk single-crystal $\text{Al}_{11}\text{Ce}_3$.

MECHANICAL PROPERTIES

Results of room-temperature mechanical property measurements are shown in Table I. Commercially pure aluminum is included from Ref. 9.

In the binary Al-12Ce sample, ductility remains high despite the large intermetallic phase fraction present in the alloy. It is not certain what mechanism enables the ductility to remain high, but this phenomenon could prove useful in applications requiring alloys to be optimized for resistance to creep failure.¹⁹ Tensile and yield strengths are improved over commercially pure aluminum (CPA). Cerium does not appear to provide dispersion strengthening in the as-cast state once heat-treated though the breakdown of the intermetallic into more particle-like structures that are on the *micrometer* scale into less coherent particles negatively effects the maximum tensile and yield strengths. The lower tensile and yield strengths are accompanied by a $\sim 100\%$ increase in ductility. This is due to a small amount of coarsening observed in the microstructure during heat-treatment. Although the coarsening is minimal because there is no diffusion into the aluminum, the bulk mechanical properties of the alloy become more similar to those of pure aluminum, with lower tensile strength and high ductility. Optimization of heat-treatment is required for the binary alloy system to limit microstructural coarsening and increase mechanical properties. The ternary Al-12Ce-0.4Mg system shows a marked increase in tensile strength over the binary alloy, which is likely due to AlMg particles dispersed throughout the aluminum matrix causing localized dislocations. However, yield strength remains relatively low. Heat-treatment again causes a decrease in yield strength and an increase in ductility. This is expected considering the similar microstructural transitions occurring in the alloys. The lower ductility results from the presence of large primary crystals, which act as nucleation sites for brittle

Table I. Room temperature mechanical properties for Al-Ce alloys

Alloy	As-cast				T6 heat-treated		
	UTS (MPa)	Yield (MPa)	Yield (4 point flexural testing)	Elongation (%)	UTS (MPa)	Yield (MPa)	Elongation (%)
CPA	90	34	—	45	—	—	—
Al-12Ce	161.3	57.2	82.0	13.5	131.7	47.6	26.5
Al-12Ce-0.4Mg	200.6	78.6	106.2	6.0	224.1	62.1	8.5
Al-12Ce-4Si-0.4Mg	141.3	75.2	155.1	2.0	252.3	128.2	8.5

fracture, and thereby decrease the overall ductility of the alloy. In contrast to the binary sample, the tensile strength is largely unaffected by heat-treatment. Although there is some difference between the heat-treated and the as-cast values, small variations between test bars could account for this change. It is then possible that the UTS is unaffected by heat-treatment.

Quaternary Al-12Ce-4Si-0.4Mg has a much more traditional response to a T6 heat-treatment than did the binary or ternary alloy. Tensile and yield strengths increased while ductility decreased. The phase transition that occurs during heat-treatment appears to be the carrier for the mechanical property increase.

CONCLUSION

Al-Ce alloys have the possibility of replacing heavier steel and cast-irons for use in high-temperature applications. Al-Ce alloys castable along a broad range of cerium content, which are compatible with modern casting practices, require no changes to the present foundry infrastructure. Mechanical properties are as high as 252 MPa for tensile and 128 MPa for yield strength. Although high-temperature mechanical properties are not represented here, the combination of thermodynamic properties and stability after heat-treatment suggest that Al-Ce-X alloys hold great promise for high-temperature mechanical properties.

Compositional variation is possible with the Al-Ce-X alloy family; Mg and Si both have the possibility to be alloyed with Al-Ce to create a highly tailorable microstructure and mechanical properties. The impediment of silicon on castability is a negative, but it is theorized that by decreasing the silicon content, good castability can be returned while maintaining the room-temperature strength of the Al-Ce-Si-Mg alloy.

ACKNOWLEDGEMENTS

This research was sponsored by the Critical Materials Institute, an Energy Innovation Hub funded by the U.S. Department of Energy, Office of Energy Efficiency and Renewable Energy, Advanced Manufacturing Office. This work was performed un-

der the auspices of the U.S. Department of Energy with Lawrence Livermore National Laboratory under Contract DE-AC52-07NA27344 and with Oak Ridge National Laboratory under U.S. Department of Energy contract DE-AC05-00OR22725. Work at the Molecular Foundry was supported by the Office of Science, Office of Basic Energy Sciences, of the U.S. Department of Energy under Contract No. DE-AC02-05CH11231. 3D printed molds and engine testing was funded by Oak Ridge National Laboratory Directed Research and Development funds. We acknowledge the support of Scott Curran and Claus Daniel with engine assembly and testing.

REFERENCES

1. Critical Materials Strategy (United States Department of Energy, 2011).
2. G.A. Gegel, *Material & Process Consultancy* (Morton, IL, 2016). Unpublished research.
3. A.A. Luo, *JOM* 54, 42 (2002).
4. J.G. Kaufman and E.L. Rooy, *Aluminum Alloy Castings: Properties, Processes, and Applications* (Materials Park, OH: ASM International, 2004).
5. L.F. Mondolfo, *Aluminum Alloys: Structure and Properties* (Atlanta, GA: Elsevier, 2013).
6. C. Booth-Morrison, D.C. Dunand, and D.N. Seidman, *Acta Mater.* 59, 7029 (2011).
7. C.B. Fuller, D.N. Seidman, and D.C. Dunand, *Acta Mater.* 51, 4803 (2003).
8. R. DeHoff, *Thermodynamics in Materials Science*, 2nd ed. (Boca Raton, FL: CRC Press, 2006).
9. S. Viswanathan, *ASM Handbook of Casting*, vol. 15, 1st ed. (Materials Park, OH: ASM International, 2008), pp. 56–63.
10. M.C. Flemings, E. Niyama, and H.F. Taylor, *AFS Trans.* 69, 625 (1961).
11. J.R. Davis, *Aluminum and Aluminum Alloys* (ASM International: Materials Park, OH, 1993).
12. D. Chakrabarti and D.E. Laughlin, *Prog. Mater. Sci.* 49, 389 (2004).
13. S.C. Bergsma, M.E. Kassner, X. Li, and M.A. Wall, *Mater. Sci. Eng. A* 254, 112 (1998).
14. Y.B. Kang, A.D. Pelton, P. Chartrand, and C.D. Fuerst, *CALPHAD* 32, 413 (2008).
15. Y. Zhong, M. Yang, and Z.K. Liu, *CALPHAD* 29, 303 (2005).
16. A.M. Samuel, J. Gauthier, and F.H. Samuel, *Metall. Mater. Trans. A* 27, 1785 (1996).
17. P. Rogl, *Ternary Alloys* vol. 5, ed. G. Petzow and G. Effenberg (Weinheim: VCH, 1991).
18. C.S. Garde, T. Takeuchi, Y. Nakano, Y. Takeda, Y. Ota, Y. Miyauchi, K. Sugiyama, M. Hagiwara, K. Kindo, F. Honda, R. Settai, and Y. Onuki, *J. Phys. Soc. Jpn.* 77, 124704 (2008).
19. J.A. Collins, *Failure of Materials in Mechanical Design: Analysis, Prediction, Prevention* (New York: Wiley, 1993).